minerals

MDPI

Article

Effect of Ordinary Portland Cement and Water Glass on the Properties of Alkali Activated Fly Ash Concrete

Vytautas Bocullo *, Danutė Vaičiukynienė, Ramūnas Gečys and Mindaugas Daukšys

Faculty of Civil Engineering and Architecture, Kaunas University of Technology, Studentų g. 48, Kaunas 51367, Lithuania; danute.vaiciukyniene@ktu.lt (D.V.); ramunas.gecys@ktu.lt (R.G.); mindaugas.dauksys@ktu.lt (M.D.)

* Correspondence: Vytautas.bocullo@ktu.lt

Received: 11 November 2019; Accepted: 24 December 2019; Published: 31 December 2019

Abstract: This research presents the influence of ordinary Portland cement (OPC) and/or water glass addition on fly ash alkali-activated mortar and concrete. The results show that fly ash (FA) concrete activated with a NaOH solution and water glass mixture had better resistance to freeze and thaw, carbonation, alkali-silica reaction (ASR) and developed higher compressive strength and static elastic modulus compared with the FA concrete activated only with an NaOH solution. The addition of OPC contributes to the development of a denser microstructure of alkali activated concrete (AAC) samples. In the presence of water glass and OPC, the compressive strength (52.60 MPa) of the samples increased more than two times as compared with the reference sample (21.36 MPa) without OPC and water glass. The combination of OPC and water glass showed the increased strength and enhanced durability of AAC. The samples were more resistant to freeze and thaw, ASR, and carbonation.

Keywords: alkali-activated concrete; fly ash; durability; compressive strength; ordinary Portland cement; industrial waste

1. Introduction

In recent years, there is more effort to make constructions more sustainable and more eco-friendly. Alkali activated concrete (AAC) is getting more attention because it has potential to reduce the use of ordinary Portland cement (OPC).

AAC is produced when aggregate particles are bound with activated aluminum and silicate raw material like fly ash (FA), blast furnace slag, and metakaolinite. Activation is achieved with alkali solution like NaOH, Na_2SiO_3, KOH, and $NaCO_3$. When raw material contacts alkali solution, the alkali activation starts. It is commonly agreed that alkali activation consists of three stages: (I) Si^{4+} and Al^{3+} ions leach from raw material (dissolution of aluminum and silicate compounds), and (II) formation of alkali activation precursors—orthosilicate phase and (III) condensation of tetrahedral consisting of 3D network of Si–O–Al framework [1–3]. The final reaction products are N–A–S–H or/and C–A–S–H gels, which are capable to bind aggregate particles [2].

AAC is an eco-friendly construction material because it can reduce the demand for Portland cement in concrete production and re-cycle industrial waste like coal combustion fly ash (FA). The annual global production of FA exceeds over 800 Mt [4] so it the most common raw material for AAC. Unfortunately, the alkali activated FA curing requires higher temperatures because then FA is more soluble [5].

Many researchers suggest increasing the calcium content in raw materials to reduce required curing temperature. The calcium content can be increased by using calcium containing FA (type C), incorporating calcium-rich initial material like blast furnace slag, or making hybrid concrete, where AAC is blended with Portland cement [5].

Portland cement presence changes the alkali activation reactions. Calcium joins the newly formed N–A–S–H (reaction (2)), which is a common reaction product of sodium aluminosilicates (lamellar or

zeolitic materials). Meanwhile the C–S–H gel, which formed during OPC hydration, goes through changes as well (reaction (1)). The gels modify in this order [6].

$$\text{C–S–H} \rightarrow \text{C–(A)–S–H} \rightarrow \text{C–A–S–H} \quad (1)$$

$$\text{N–A–S–H} \rightarrow \text{(N,C)–A–S–H} \rightarrow \text{C–A–S–H} \quad (2)$$

As seen in the transformations above, calcium, which was applied in the system with OPC, modifies the N–A–S–H gel where it replaces sodium as a charge-balancing cation forming a (N,C)–A–S–H gel [7,8], which gradually transforms into C–A–S–H. The transformation continues until there is enough calcium content [6]. It is reported that AAC blended with Portland cement has a higher compressive strength, elastic modulus, more rapid curing, and lower water absorption porosity [5,7,9–11]. Due to the previously mentioned parameters, the blended AAC has better resistance to chloride penetration and repetitive freeze–thaw cycles, according to Nuaklong et al. [11]. The enhanced properties can be attributed to the denser microstructure of C–A–S–H gel compared to N–A–S–H, which is the product of FA alkali activation. Additionally, C–A–S–H, which has a higher chloride binding capacity than 3D-polymeric structure like N–A–S–H phases.

Despite all benefits, there are some negative aspects that have to be considered. First, the reduction of mixture workability was noted nearly in every case study [5,11]. In addition, Nuaklong [11] reports that systems containing C–A–S–H decomposed more under Sulphur attack compared to the systems dominated by N–A–S–H.

The presence of calcium in alkali-activated systems such as alkali-activated materials can possibly lead to alkali-silica reaction (ASR). AAC is known to be resistant to ASR if the aggregate contains reactive rocks [12–14]. When calcium is present, deterioration can occur involving formation of alkali-silica gel near reactive aggregates, which causes expansion and cracking. Bakharev [15] investigated ASR in slag AAC and concluded that alkali-activated slag is more susceptible to deterioration from ASR than OPC of similar grade. Tänzer [16] reveals that high inherent alkali content of alkali activated slag can result in the risk of ASR. Both studies produced concrete by activating blast furnace slag, which is material consisting of CaO by nearly 40%. On the other hand, Shi [14] investigated the effect of alkali dosage on ASR in alkali-activated slag and concluded that alkali-activated slag shows relatively better performance compared to OPC containing the same aggregate. The author attributed resistance to the lower alkalinity of the pore solution of the AAC than OPC after 28 days of exposure to 1 mol/L NaOH solution, even though the alkalinity of the pore solution is higher for AAC than for OPC before exposing to NaOH solution.

There are undoubtedly certain contradictions in the ASR research. In order to make clear conclusions, more investigations should be carried out. The aim of this work is to investigate the effect of OPC or/and water glass addition on the mechanical and durability properties of alkali activated fly ash mortar and concrete.

2. Materials and Methods

2.1. Experimental Techniques

The X-ray diffraction (XRD) analysis was performed on the D8 Advance diffractometer (Bruker AXS, Karlsruhe, Germany) operating at the tube voltage of 40 kV and tube current of 40 mA. The X-ray beam was filtered with a Ni 0.02-mm filter to select the CuKα wavelength. The powder X-ray diffraction patterns were identified with references available in the PDF-2 database.

X-ray fluorescence (XRF) was performed on an X-ray fluorescence spectrometer Bruker X-ray S8 Tiger WD (Bruker, Billerica, MA, USA). The Rh tube, anode voltage U_a up to 60 kV, and current I to 130 mA were used. The loss on ignition was calculated after heating the materials at the temperature of 1000 °C.

The normal consistency of fresh alkali activated fly ash paste, which was determined by Suttard's viscometer. The fineness of OPC and fly ash was evaluated by the Blaine method.

The AAC samples were 70 × 70 × 70 mm cubes and mortar samples were 40 × 40 × 160 mm prisms samples. There were three samples of the same composition for each test. Different sample sizes were required for different tests. These samples were sealed in molds after formation and kept at an ambient temperature for 24 h. The samples were then moved to 60 °C for 24 h. After the curing period, they were demolded, dried, and left at room temperature for 26 days.

The compressive strength test was carried out on the concrete cubes after 7, 14, and 28 days. The hydraulic compression machine Toni Technik 2020 (Toni Technik GmbH, Berlin, Germany) was used for the test.

Elastic modulus was determined, according to standard ISO 1920-10:2010. During the test, the mortar prisms were placed in a frame and loaded by 40% of their destructive load for three times, and strains and deformations were monitored during loading/unload. The static elastic modulus was calculated as follows.

$$E = \frac{\sigma_a - \sigma_b}{\varepsilon_a - \varepsilon_b} \cdot 100 \quad (3)$$

where E—elasticity module, MPa; σ_a—Maximum load (40% $F_{C,Cub.}$—previously determined compressive strength), MPa; σ_b—minimum load (≈ 0.5 MPa), MPa; ε_a—relative deformation at maximum load; and ε_b—relative deformation at the lowest load.

Carbonation of AAC was evaluated by measuring the depth of the carbonated layer. The initial carbonation depth was measured in the 28-day-old sample and compared with the depth after keeping samples in a carbonation chamber for 56 days (CO_2 concentration 1%, temperature 20 °C). In order to measure the carbonation depth, the samples must be split and sprayed with phenolphthalein solution. Then the uncarbonated layer turns into a purple color.

Porosity was determined by using the water absorption kinetics test. For each type of sample, the experiment was repeated at least three times. In order to calculate the total porosity, open porosity, closed porosity, the dry sample mass, the sample mass after 48 h of drowning, and the sample mass in the water must be measured. The sample density is calculated below.

$$\rho = \frac{m_d}{m_{48} - m_w} \cdot 1000,\ kg/m^3 \quad (4)$$

Here, m_{48}—sample mass after 48 h of drowning, g; m_d—dry sample mass, g; and m_w—sample mass in the water (after 48 h drowning), g.

Water volume absorption ($W_{p(t)}$) of the sample is equal to open porosity (P_o).

$$P_o = W_{p(t)} = \frac{W_p \rho}{1000},\ \% \quad (5)$$

Here: W_p—water mass absorption, %, ρ—density, kg/m^3.

Porosity can be calculated with the following equation.

$$P = \left(1 - \left(\frac{\rho}{2690}\right)\right) \cdot 100, \% \quad (6)$$

Here: ρ—density, kg/m^3, and 2690 kg/m^3 is theoretical concrete density, according to standard GOST 12730.4-78.

Then the closed porosity (P_c) is equal to:

$$P_c = P - P_o,\ \% \quad (7)$$

To measure the danger of ASR, the test was carried out, according to standard RILEM AAR-2. During the test, 40 × 40 × 160 mm prisms are placed in 1 mol/L NaOH in an 80 °C solution, and measured after one, three, seven, and 14 days. Deformations are recalculated into relative deformations.

According to the regulations of standard ASTM C1260, concrete is resistant to ASR when relative deformations are under 1 mm/1 m after 14 days.

Resistance to freeze/thaw was evaluated with a testing method regulated by standard SS 137244:2005. According to the regulations, the top surface of the samples is exposed to an NaCl solution (concentration 3%) and cycles of freeze/thaw (from −20 to +20 °C) are applied for 56 days (chamber does one cycle per day). Other surfaces are insulated from the effect. After 56 days, the mass loss from the affected sample is measured. According to the regulations of standard SS 137244:2005, the mass loss must be under 1 kg/m^2.

For each test, at least three samples were used.

2.2. Materials and Sample Preparation

Fly ash type F is considered to be an excellent material to synthesize alkali-activated materials [17, 18]. With reference to XRD analysis (Figure 1), the peaks of quartz (78-1252) and mullite (79-1454) refer to the major crystalline minerals of this material. High amounts of amorphous SiO_2 and Al_2O_3 make FA the right raw material for alkali-activated binders (Table 1). The bulk density of the F Class FA that was used in the research is 1.84 g/cm^3 and it was determined by the helium pycnometer "Quantachrome Multi Pycnometer" (Quantachrome GmbH & Co. KG, Odelzhausen, Germany).

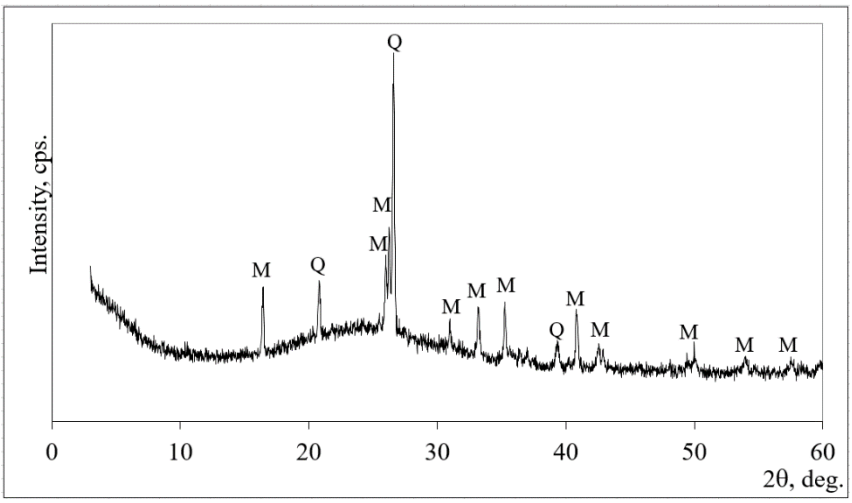

Figure 1. XRD analysis of used fly ash. Q—quartz (78-1256); M—mullite (73-1253).

Table 1. Chemical composition of fly ash and ordinary Portland cement.

Oxide	CaO	SiO_2	Al_2O_3	Fe_2O_3	K_2O	MgO	SO_3	Na_2O	TiO_2	ZrO_2	ZnO	MnO	Others
FA	3.68	49.47	27.45	7.38	4.54	1.70	0.92	0.95	1.66	0.147	0.05	0.063	1.99
OPC	61.32	19.51	5.25	3.36	1.01	3.84	4.30	0.94	0.13	0.016	-	0.042	0.282

In this study, commercial ordinary Portland cement (OPC) of type CEM I 52.5R was used for the tests. Chemical composition of Portland cement is shown in Table 1.

As the alkaline activator, the mixture of sodium silicate hydrate (water glass) and sodium hydroxide (NaOH) solution were used. Water glass (Silpur, Poland) with silicate modulus 3.0 and specific gravity of 1.42 g/mL was used in these experiments. Commercial sodium hydroxide NaOH pellets (99% purity, Eurochemicals) were used for the preparation of the alkaline solutions.

NaCl solution (Lach-Ner, Czech Republic) was used for evaluating resistance to freeze/thaw.

As a chemical admixture, the superplasticizer Schomburg Remicrete SP 56 (FM) based on the modified polymers compound was used. The dosage was 0.7% from binder mass (FA mass, FA, and OPC mass) as recommended by the manufacturer.

The sand (0/4 fraction) was used as a fine aggregate from Kvesai quarry (Lithuania). As a coarse aggregate, the granite macadam (4/16 fraction) was used. The waste glass was crushed by the glass bottle to obtain particle sizes with the fraction 4/2 (Table 2). This waste glass cullet was used to investigate the AAC samples expansion due to ASR.

Table 2. The compositions (kg) for 1 m^3 concrete mixtures.

Ingredients	NaOH Activation		NaOH + $Na_2OnSiO_2 \cdot mH_2O$ Activation	
	0NS0PC	**0NS15PC**	**50NS0PC**	**50NS15PC**
Sand 0/4	583 *	583 *	583 *	583 *
Sand 0/4	1312 **	1312 **	1312 **	1312 **
Sand 0/4	1180 ***	1180 ***	1180 ***	1180 ***
Gravel 4/16	729 *	729 *	729 *	729 *
Gravel 4/16	0 **	0 **	0 **	0 **
Gravel 4/16	0 ***	0 ***	0 ***	0 ***
Water	238	238	119	119
FA	719	611	719	611
NaOH	166	166	83	83
Water glass	0	0	202	202
OPC	0	108	0	108
Glass cullet (4/2)	131 ***	131 ***	131 ***	131 ***
Superplasticizer	0	0	0	13

Notes: Superplasticizer is Remicrete SP 56; *: amount for concrete mixture; **: amount for mortar mixture; ***: amount for special mixture for ASR test.

In order to investigate the influence of OPC, four different mixtures were designed. The first mixture is marked 0NS0PC and it is FA activated with NaOH solution. No additional OPC and no water glass. The second mixture (0NS15PC) is fly ash with 15% of the mass replaced by OPC and activated by NaOH solution. The composition of mixtures 50NS0PC and 50NS15PC has the same raw materials. Only the activator solution consists of NaOH and the water glass mixture (Table 2).

According to the Suttard's viscometer experimental results, the consistency of alkali-activated fly ash paste strongly depends on using the water glass. In these cases, the consistency values were 200 mm and 135 mm (Figure 2).

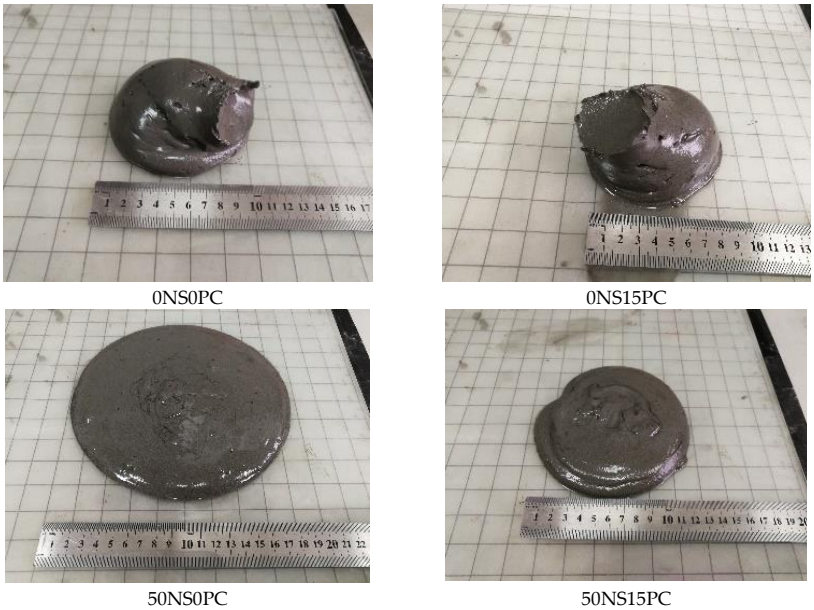

Figure 2. The flow characteristics (consistence, mm) of the alkali-activated fly ash pastes.

In pastes without a water glass, pastes spread only for 100 and 95 mm. The addition of OPC had a significant influence on alkali-activated fly ash pastes with the water glass. However, without the water glass, the influence was insignificant (Figure 2). This could be explained by the specific surface area of OPC and fly ash. The specific surface area of fly ash is 28.07 m^2/g and the surface area for OPC is 35.60 m^2/g (Blaine). The pastes containing a finer fraction of OPC occupied a lager specific surface area (35.60 m^2/g) as compared with fly ash. Therefore, it required more water to lubricate the particle surface, and, thus, it exhibited less consistency values. Similar results were published by Samantasinghar et al. [19].

3. Results and Discussion

3.1. Mechanical Properties

Different compositions resulted in very different compressive strengths (Figure 3a). Surprisingly, 0NS0PC samples achieved a higher compressive strength value (21.4 MPa) than the samples with additional OPC (0NS15PC) of 17.51 MPa, despite the fact that the sample density of 0NS15PC was higher at 2084 kg/m^3, when 0NS0PC was 2043 kg/m^3. The negative effect of OPC additive contradicts with the previous work carried out using the alkali activated mortar with the OPC additive [20]. The contributed factors could be different curing conditions if compared to our previous work [21]. The mortar samples were cured at elevated temperatures for the entire duration of the experiment (28 days), while concrete was cured at 60 °C only for 48 h.

Despite the fact that the samples activated with NaOH and water glass (50NS0PC and 50NS15PC) solution samples were less dense, i.e., 1923 kg/m^3 and 1938 kg/m^3, respectively, the compressive strength after 28 days was much higher at 36.1 MPa (50NS0PC) and 52.6 MPa (50NS15PC) (Figure 3a) as compared with the samples without OPC. 50NS0PC samples (without additional OPC) achieved compressive strength after 28 days within the first seven days and it stayed at around 35 MPa. The compressive strength of 50NS15PC samples was growing gradually throughout the curing period. It can be explained by the fact that, during the alkali activation process, the additional amount of C–S–H gel form by hydration of OPC. The elastic modulus of 50NS15PC reached the highest values as well as compared with other compositions of 14 GPa (Figure 3b). The presence of water glass had a positive effect on static elastic modulus.

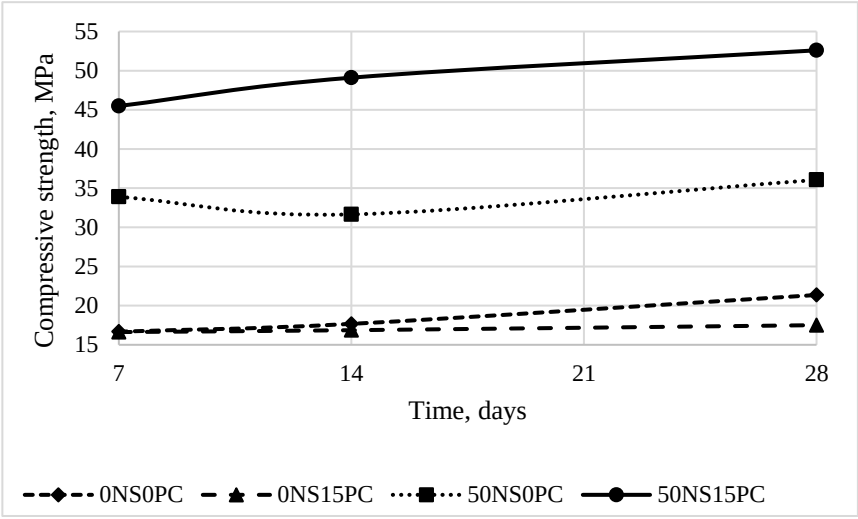

(**a**)

Figure 3. *Cont.*

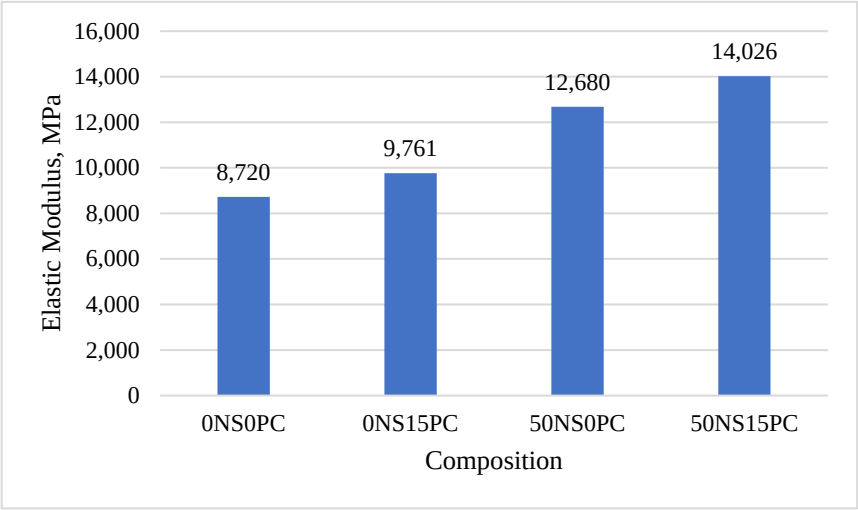

(**b**)

Figure 3. Concrete compressive strength development of concrete samples (**a**) and static elastic modulus of alkali-activated mortar prisms (**b**).

3.2. Porosity

Porosity is one of the main durability defining factors. Smaller open porosity means that a smaller amount of potentially dangerous compounds can penetrate deep into the concrete structure. In this case, OPC and water glass changed the microstructure of the sample and porosity (Figure 4). The porosity of 0NS0PC concrete was 28.1%, the closed porosity was 10.9%, the porosity of 0NS15PC was 26.9%, and the closed porosity was 7.7%. It can be concluded that the presence of OPC reduced porosity. The porosity of 50NS0PC was 28.5% and the closed porosity was 11.3, which shows that porosity is slightly higher with the water glass. The porosity of 50NS15PC was 27.95% and closed porosity was 9.6%, which is slightly less than 50NS0PC. This indicates that OPC is balancing the effect of water glass on porosity.

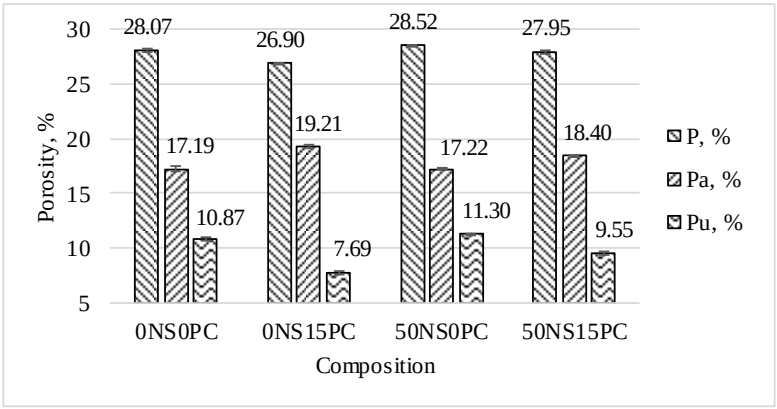

Figure 4. AAC samples porosity. P—total porosity; Pa—open porosity; Pu—closed porosity.

3.3. Durability of Alkali-Activated Materials

The deformations in ASR strongly depended on the composition of the activator solution (Figure 5). The samples activated with NaOH expanded relatively rapidly: after one day, relative deformations reached 1.41 mm/1 m in 0NS0PC compositions, and relative deformations reached 1.55 mm/1 m in 0NS15PC composition. During the following days, the samples deformed very little.

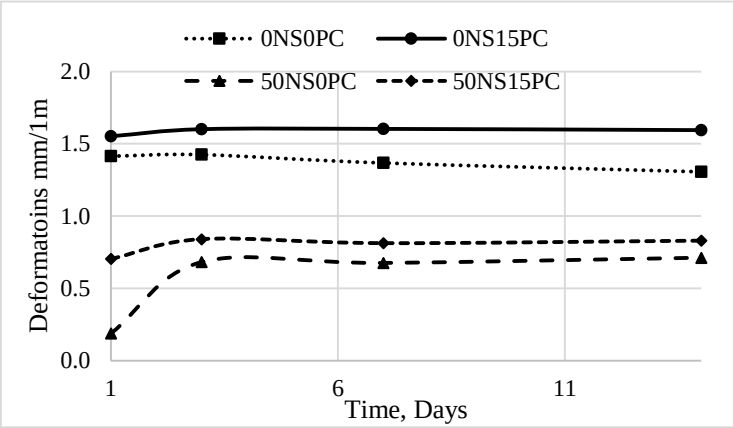

Figure 5. AAC samples expansions due to ASR.

The samples with water glass in the activator solutions (compositions 50NS0PC and 50NS15PC) expanded much less when compared with the samples without water glass. The results were 0.71 mm/1 m and 0.83 mm/1 m, respectively, after 14 days of the experiment (Figure 5). The expansions of the samples 50NS0PC and 50NS15PC were under 1.0 mm/1 m, which is acceptable by the regulations RILEM AAR-2. It is worth mentioning that even 0NS0PC and 0NS15PC composition samples had relatively big expansions, but there were no ASR signs visually, such as crack network or local pop-outs [21]. In addition, the surface was smooth.

It appears that the presence of OPC increases the resistance of AAC to freeze and thaw cycles. When OPC is absent, the mass loss of the samples with FA concrete activated with NaOH and NaOH with water glass mixture were more than 1 kg/m^2, namely, 1571 g/m^2 and 1265 g/m^2 (Figure 6). For FA concrete activated with NaOH, the amount of OPC necessary to reduce mass loss to under 1000 g/m^2 was 10%, while concrete activated with NaOH and water glass was 5%. The effect of OPC on increased resistance to freeze/thaw cycles can be attributed to the reduced porosity. Additionally, the addition of water glass makes concrete much stronger. Therefore, it can better withstand internal tensions due to ice expansions.

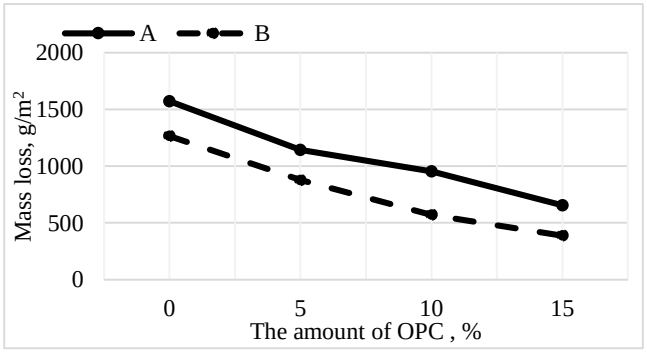

Figure 6. Additional OPC influence on alkali-activated concrete resistance to repetitive freeze/thaw. Notes: A—FA + NaOH; B—NaOH + Na_2SiO_3.

The carbonation process can negatively affect the development of the mechanical strength of AAC and could be the reason for reinforcement corrosion in the concrete [22,23]. During the carbonation process, the pH modifies the kinetic rate of the hydration reactions of AAC. Consequently, the initial carbonation is closely related to the reduction of the pH values of AAC. For this reason, the mechanical properties and hydration rate of AAC decreased.

The OPC effect on carbonation was clear after measuring the depth of the carbonated layer. The samples possessing OPC in the composition showed a shallower carbonated layer. The initial carbonation layer of the 28 day old samples without OPC (0NS0PC) was 4 mm. After 56 days of the

samples' exposure to CO_2 in the carbonation chamber, this layer reached 25 mm (Figure 7a). Meanwhile, after the initial 28 days, AAC samples with 15% OPC were significantly less affected by CO_2 compared with other compositions, and the depth of carbonation reached 2.5 mm after 56 days of exposure to CO_2 in the chamber (Figure 7b). This low rate of carbonation could be related to the physical properties of the samples: the low porosity and the high density. The water glass increased the rate of carbonation. The initial carbonated layer reached 7.5 mm deep and, after 56 days of exposure to CO_2, it was 23.5 mm. When OPC is used together with water glass, it balances the system. The carbonation was initially at 4.5 mm and, after 56 days, the period of exposure to CO_2 reached only 10.5 mm (Figure 7a,b).

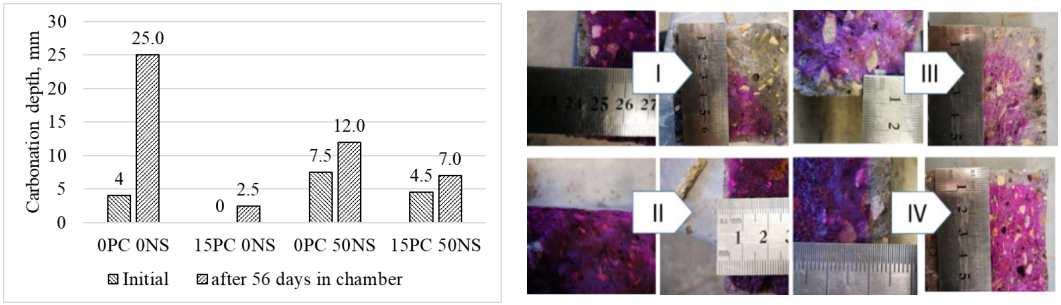

(**a**) (**b**)

Figure 7. The depth of AAC samples carbonation (**a**) and the samples after carbonation tests (**b**). Notes: I—0NS0PC, II—0NS15PC, III—50NS0PC, IV—50NS15PC and the pink zones are uncarbonated parts of the samples. The initial depth was measured after 28 days in room conditions and then samples were treated in a carbonation chamber for 56 days.

4. Conclusions

AAC was activated with NaOH and the water glass mixture had better resistance to freeze and thaw, carbonation, and ASR. In addition, it developed a higher compressive strength. In the presence of water glass, OPC can participate in the development of compressive strength. The compressive strength of the samples with OPC additive but without water glass was 17.51 MPa. At the same time, the compressive strength of the samples with water glass in the activator solution was 52.6 MPa. Furthermore, the mixture starts binding at an ambient temperature. When OPC is used as an additive, a denser structure forms, which compensates for the effect of water glass. Due to these reasons, it is beneficial to use OPC with the water glass.

1. The expansive deformations are less significant when there are conditions promoting ASR.
2. Carbonation depth is reduced.
3. The amount of material detached due to repetitive freeze and thaw is reduced.

Author Contributions: Conceptualization, D.V. and M.D.; Methodology, M.D.; Validation, R.G. and V.B.; Formal Analysis, D.V. and V.B.; Investigation, V.B.; Resources, R.G. and V.B.; Data Curation, V.B.; Writing—Original Draft Preparation, V.B.; Writing—Review & Editing, D.V., M.D., V.B. and R.G.; Visualization, V.B.; Supervision, M.D.; Project Administration, D.V.; All authors have read and agreed to the published version of the manuscript.

Funding: This research received no external funding.

Conflicts of Interest: The authors declare no conflict of interest.

References

1. Król, M.; Ro, P.; Chlebda, D.; Mozgawa, W. Molecular and Biomolecular Spectroscopy In fl uence of alkali metal cations/type of activator on the structure of alkali-activated fly ash—ATR-FTIR studies. *Spectrochim. Acta Part A* **2018**, *198*, 33–37. [CrossRef] [PubMed]
2. Khalid, H.R.; Lee, N.K.; Park, S.M.; Abbas, N.; Lee, H.K. Synthesis of geopolymer-supported zeolites via robust one-step method and their adsorption potential. *J. Hazard Mater.* **2018**, *353*, 522–533. [CrossRef] [PubMed]
3. Rozek, P.; Krol, M.; Mozgawa, W. Geopolymer-zeolite composites: A review. *J. Clean. Prod.* **2019**, *230*, 557–579. [CrossRef]
4. Belviso, C. State-of-the-art applications of fly ash from coal and biomass: A focus on zeolite synthesis processes and issues. *Prog. Energy Combust. Sci.* **2018**, *65*, 109–135. [CrossRef]
5. Askarian, M.; Tao, Z.; Adam, G.; Samali, B. Mechanical properties of ambient cured one-part hybrid OPC-geopolymer concrete. *Constr. Build. Mater.* **2018**, *186*, 330–337. [CrossRef]
6. Garcia-Lodeiro, I.; Palomo, A.; Fernández-Jiménez, A.; Macphee, D.E. Compatibility studies between N–A–S–H and C–A–S–H gels, Study in the ternary. *Cem. Concr. Res.* **2011**, *41*, 923–931. [CrossRef]
7. García-Lodeiro, I.; Maltseva, O.; Palomo, Á.; Fernández-Jiménez, A.N.A. Cimenturi hubride alcaline partea I: Fundamente. Hybrid alkaline cements. *Rev. Romana Mater.* **2012**, *42*, 330–335.
8. Palomo, A.; Krivenko, P.; Kavalerova, E.; Maltseva, O. A review on alkaline activation: New analytical perspectives. *Mater. Construcción* **2018**, *64*, 22. [CrossRef]
9. Nath, P.; Sarker, P.K. Use of OPC to improve setting and early strength properties of low calcium fly ash geopolymer concrete cured at room temperature. *Cem. Concr. Compos.* **2015**, *55*, 205–214. [CrossRef]
10. Nath, P.; Sarker, P.K. Flexural strength and elastic modulus of ambient-cured blended low-calcium fly ash geopolymer concrete. *Constr. Build. Mater.* **2017**, *130*, 22–31. [CrossRef]
11. Nuaklong, P.; Sata, V.; Wongsa, A.; Srinavin, K.; Chindaprasirt, P. Recycled aggregate high calcium fly ash geopolymer concrete with inclusion of OPC and nano-SiO_2. *Constr. Build. Mater.* **2018**, *174*, 244–252. [CrossRef]
12. Pouhet, R.; Cyr, M. Alkali—silica reaction in metakaolin-based geopolymer mortar. *Mater. Struct.* **2015**, *48*, 571–583. [CrossRef]
13. Kupwade-Patil, K.; Allouche, E. Effect of Alkali Silica Reaction (ASR) in Geopolymer Concrete. In Proceedings of the World of Coal Ash (WOCA) Conference, Denver, CO, USA, 9–12 May 2011.
14. Shi, Z.; Shi, C.; Wan, S.; Ou, Z. Effect of alkali dosage on alkali-silica reaction in sodium hydroxide activated slag mortars. *Constr. Build. Mater.* **2017**, *143*, 16–23. [CrossRef]
15. Bakharev, T.; Sanjayan, J.G.; Cheng, Y. Resistance of alkali-activated slag concrete to alkali—Aggregate reaction. *Cem. Concr. Res.* **2001**, *31*, 331–334. [CrossRef]
16. Tänzer, R.; Jin, Y.; Stephan, D. Effect of the inherent alkalis of alkali activated slag on the risk of alkali silica reaction. *Cem. Concr. Res.* **2017**, *98*, 82–90. [CrossRef]
17. Riahi, S.; Nazari, A.; Zaarei, D.; Khalaj, G.; Bohlooli, H.; Kaykha, M.M. Compressive strength of ash-based geopolymers at early ages designed by Taguchi method. *Mater. Des.* **2012**, *37*, 443–449. [CrossRef]
18. Lloyd, N.A.; Rangan, B.A. Geopolymer Concrete with Fly Ash. In Proceedings of the Second International Conference Sustainable Construction Materials and Technologies, Ancoma, Italy, 28–30 June 2010; pp. 1493–1504.
19. Samantasinghar, S.; Singh, S.P. Hardened Properties of Fly Ash–Slag Blended Geopolymer Paste and Mortar. *Int. J. Concr. Struct. Mater.* **2019**, *13*, 47. [CrossRef]
20. Bocullo, V.; Vaičiukynienė, D.; Borg, R.P.; Briguglio, C. Alkaline Activation of Hybrid Cements Binders Based on Industrial by-Products. *J. Sustain. Archit. Civ. Eng.* **2017**, *19*, 65–73.
21. Grinys, A.; Bocullo, V.; Gumuliauskas, A. Research of Alkali Silica Reaction in Concrete With Active Mineral Additives. *J. Sustain. Archit. Civ. Eng.* **2014**, *6*, 34–41. [CrossRef]
22. Puertas, F.; Palacios, M.; Vázquez, T. Carbonation process of alkali-activated slag mortars. *J. Mater. Sci.* **2006**, *41*, 3071–3082. [CrossRef]
23. Alaa, M. A synopsis of carbonation of alkali-activated materials. *Greem Mater.* **2019**, *7*, 1–19.